Virology 501 (2017) 25–34

Contents lists available at ScienceDirect

Virology

journal homepage: www.elsevier.com/locate/yviro

Elevating fitness after a horizontal gene exchange in bacteriophage φX174

Sarah M. Doore[1], Nicholas J. Schweers, Bentley A. Fane*

School of Plant Sciences and the BIO5 Institute University of Arizona, Tucson, AZ 85721, USA

ARTICLE INFO

Keywords:
φX174
Microviridae
Microvirus
Experimental evolution
Virus assembly

ABSTRACT

In an earlier study, protein-based barriers to horizontal gene transfer were investigated by placing the bacteriophage G4 G gene, encoding the major spike protein, into the φX174 genome. The foreign G protein promoted off-pathway assembly reactions, resulting in a lethal phenotype. After three targeted genetic selections, one of two foreign spike proteins was productively integrated into the φX174 system: the complete G4 or a recombinant G4/φX174 protein (94% G4:6% φX174). However, strain fitness was very low. In this study, the chimeras were characterized and experimentally evolved. Inefficient assembly was the primary contributor to low fitness: accordingly, mutations affecting assembly restored fitness. The spike protein preference of the ancestral and evolved strains was determined in competition experiments between the foreign and φX174 G proteins. Before adaptation, both G proteins were incorporated into virions; afterwards, the foreign proteins were strongly preferred. Thus, a previously inhibitory protein became the preferred substrate during assembly.

1. Introduction

Horizontal gene transfer (HGT) occurs extensively between viruses (Diemer and Stedman, 2012; Gibbs and Weiller, 1999; Hendrix et al., 1999; Roux et al., 2012), yet relatively few recombinants persist in nature (Lefeuvre et al., 2007). To persist, new recombinants must be able to immediately compete or be in an environment that favors further adaptation. For example, environments with high viral densities can provide less fit variants or recombinants with helper viruses that supply necessary proteins and other resources (Froissart et al., 2004; Montville et al., 2005; Wichman et al., 2005).

Bacteriophages T7, φ6 and the microviruses (canonical members φX174, G4 and α3), have emerged as powerful experimental evolution systems (Burch and Chao, 1999; Cecchini et al., 2013; Froissart et al., 2004; Montville et al., 2005; Springman et al., 2012; Wichman et al., 1999, 2005). When genes encoding virion structural proteins are exchanged between microviruses, the new recombinants exhibit significantly lower fitness than their respective parental strains (Doore and Fane, 2015, 2016; Rokyta and Wichman, 2009; Sackman et al., 2015; Sackman and Rokyta, 2013). In these studies, particle assembly is the major contributing factor to fitness loss. Once assembled, particles appear to function efficiently vis-à-vis their ability to recognize and penetrate host cells. Accordingly, fitness recovery is often achieved by mutations affecting scaffolding protein interactions.

Microvirus assembly requires two scaffolding proteins that divide the morphogenetic pathway into early and late stages (Fig. 1A). The early stage is mediated by the internal scaffolding protein B. Five copies of B protein, along with one copy of DNA pilot protein H, bind to the underside of the 9 S coat protein F pentamer to produce the 9 S* particle. B protein induces a conformational change that facilitates interactions between the coat and the 6 S major spike protein G pentamer (Gordon et al., 2012). This joining of the 6 S pentamer to the top of the 9 S* intermediate produces the 12 S* particle (Cherwa et al., 2008). The second stage of assembly occurs when 240 copies of external scaffolding protein D organize twelve 12 S* particles into a procapsid (Cherwa et al., 2011). At this point, packaging of the genome occurs with the concurrent loss of internal scaffolding protein. With the release of the external scaffolding protein, the capsomeres undergo a radial collapse to produce the mature virion (Dokland et al., 1997; Hafenstein and Fane, 2002; McKenna et al., 1994).

In a previous study (Doore and Fane, 2015), the major spike gene G was exchanged between φX174 and G4 to produce φXG4G and G4φXG. The primary consequence of this horizontal gene transfer was an elevated activation energy during one or more assembly reactions. The size of this barrier depended on the direction of gene transfer: for G4φXG, the new gene was tolerated but displayed a temperature sensitive assembly defect. This was corrected via second site suppressors affecting internal scaffolding protein interactions. By contrast, φXG4G exhibited a lethal phenotype. Viability required the exogenous expression of *two* cloned φX174 genes, G and H. The latter

* Correspondence to: The BIO5 Institute, The University of Arizona, 1657 E. Helen Street, Tucson, AZ 85721.
E-mail address: bfane@email.arizona.edu (B.A. Fane).
[1] Present address: Department of Biochemistry and Molecular BiologyMichigan State UniversityBiochemistry Building603 Wilson RoadEast Lansing, MI 48824

http://dx.doi.org/10.1016/j.virol.2016.10.029
Received 5 September 2016; Received in revised form 11 October 2016; Accepted 30 October 2016
Available online 14 November 2016
0042-6822/

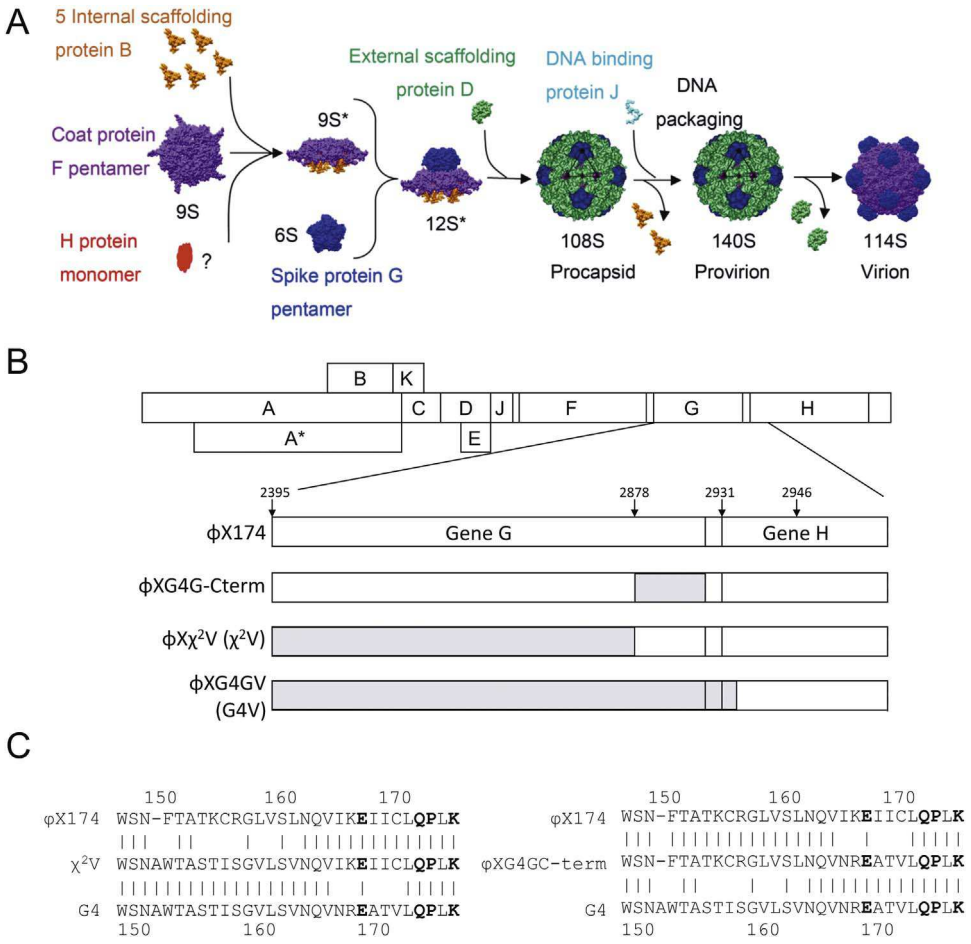

Fig. 1. A) the microvirus assembly pathway. B) the linear microvirus genome with simplified diagrams of the chimeric major spike G genes described in this study. Due to a recombination event (see text for details), the first eight amino acid residues of the H protein in φXG4GV are derived from G4. The first 20 amino acids of gene H encode a strongly conserved transmembrane helix. C) Protein alignment of the C-terminus of the major spike genes encoded by χ^2V (left) and φXG4Cterm (right) mutants. The conserved amino acid residues that mediate F-G interactions are in bold text.

gene encodes the DNA pilot protein, which is produced at the lowest quantity of all structural proteins during an infection. The foreign G4 G protein interacted non-productively with the φX174 H protein or an H protein-containing intermediate, effectively removing this protein from the productive assembly pathway. Thus, an additional supply of the H protein, as well as the indigenous G protein, was required for plaque formation.

After three targeted genetic selections, viable φXG4G chimeras were recovered. The initial chimera required the exogenous expression of both the φX174 G and H genes to form plaques (Doore and Fane, 2015). In the first selection, variants that no longer required exogenous H gene expression were recovered. This first adaptation suppressed non-productive interactions between the foreign G protein and the indigenous H protein. This was achieved via two changes. First, a truncated version of the C protein, which partially mediates the balance between DNA replication and transcription, resulted in global down-regulation of all viral genes. In addition, a recombination event between the genome-encoded G4 and plasmid-encoded φX174 G genes resulted in a chimeric major spike gene (χ^2: chimeric gene in chimeric genome). 94% of the genomic gene was derived from G4, while the 3′ 6%, which encodes the C-terminus, was φX174 in origin (Fig. 1B,C). X-ray models indicate that the coat F and major spike G proteins are nearly superimposable across the three microvirus clades (Bernal et al., 2003; McKenna et al., 1996, 1992). The interactions between these two proteins are primarily mediated by conserved residues in the C-terminus of the major spike protein (bold text, Fig. 1C). Although the interacting amino acid residues are conserved, five of the fourteen C-terminal amino acids differ between species, potentially altering these interactions.

In the second selection, subsequent adaptations of the φXG4G chimera affected key protein-protein interactions that govern assembly. In this selection, mutants capable of forming plaques on cells expressing the G4 G gene were isolated. These mutants still required exogenous G gene expression, but the expressed gene could be from either φX174 or G4. Most of the mutations involved interactions with the external scaffolding protein. In the third selection, two complementation-independent viable chimeras were recovered. These two mutants were able to form plaques without any exogenous G gene expression. One retained the chimeric major spike gene (φXχ^2V or χ^2V) but acquired additional mutation in the F-G intercistronic region. The other underwent another recombination event, restoring the full-length genomic G4 major spike gene (φXG4GV or G4GV). Simplified diagrams of the viable chimeras' G genes are illustrated in Fig. 1B and the lineage of the strains used these studies is given in Fig. 2. Both complementation-independent chimeras exhibited low fitness. Throughout the previous study, the χ^2V major spike protein was hypothesized to be a less-fit hybrid. The present study investigates this possibility further. First, both chimeras were characterized in terms of assembly and function. These strains were then experimentally evolved to determine how fitness could be recovered. In addition, we engineered and examined the reciprocal of the χ^2V recombination pattern in the φX174 background. This chimeric major spike protein is 94% φX174, with the C-terminal 6% encoded by G4 (φXG4GC-term; Fig. 1C). This allowed us to examine the specific defect(s) conferred

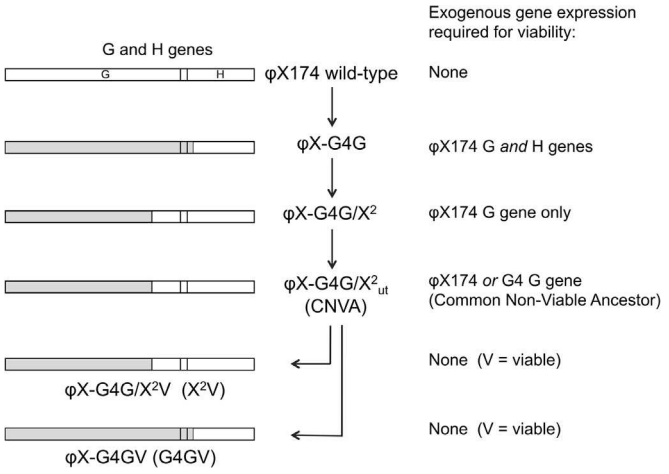

Fig. 2. Flow chart representing critical stages during the evolution of the viable chimeras. The G and H genes of each mutant stage are represented on the left using the schematic of Fig. 1. Note that the full length of gene H is not shown. Genes required for complementation are indicated on the right, along with defined abbreviations.

by the non-conserved C-terminal residues.

2. Results and discussion

2.1. Chimeric particles exhibit delayed assembly and attachment kinetics

The φXG4G/χ^2V and φXG4GV chimeras, hereafter referred to as χ^2V and G4GV, formed very small plaques and exhibited fitness values significantly lower than wild-type φX174 (Table 1). To investigate the potential defect(s) resulting in low fitness, the kinetics of assembly, attachment, and eclipse were investigated. Attachment for both chimeras was modestly but significantly delayed compared to wild-type (Fig. 3A). Wild-type particles reach 90% attachment after approximately 3 min and approach 99% by 12 min, whereas only 70% of the G4GV and χ^2V chimeric particles had attached by 3 min. The chimeras did not reach 90% attachment until 9 min, demonstrating an approximate 6 min lag behind wild-type. Once attached, eclipse kinetics did not differ from wild-type (data not shown).

Two protocols were used to investigate assembly kinetics of the viable chimeras. To control for the potential effects arising from less efficient attachment, phage were pre-attached to lysis resistant cells in the first protocol. By contrast, the second protocol was designed to mimic the conditions used in fitness assays, in which virions are not pre-attached. The inclusion of the pre-attachment in the first protocol had little or no effect on the experimental results: thus, only the results from the second protocol are presented (Fig. 3B). Both chimeras exhibited delayed kinetics and/or inefficient particle production. In these assays, wild-type progeny production increased steeply 15–20 min post infection. Although the G4GV chimera produced a modest amount of progeny during this period, particle production did not increase steeply until 20–25 min post infection. Conversely, the χ^2V chimera exhibited a significantly longer lag phase, producing progeny between 25 and 30 min post infection. The statistically most significant time points were at 20 and 25 min (see figure legend for details).

Attachment defects were not anticipated based on results from the previous study (Doore and Fane, 2015). In that study, a reciprocal chimera, G4φXG, was examined. This chimera encoded the φX174 major spike G gene in the G4 genome. Although it exhibited slower assembly kinetics, virions displayed wild-type attachment kinetics. Delayed assembly defects in the G4φXG chimera were corrected by single mutations. By contrast, when the G4 G gene was placed into the φX174 background, this φXG4G chimera required multiple mutations to form plaques at any temperature. With greater barriers to productive

Table 1
Mutations of ancestral and evolved strains.

Strain	Fitness[a]	G protein[b]	Genotypic changes[c]: Nucleotide	Amino acid	Hypothesized Function and/or structural contacts[d]
G4 WT	13.7 ± 0.3	WT G4			
φX WT anc.	14.2 ± 1.3	WT φX			
φX WT ev-o1	13.3 ± 0.1	WT φX	A2166G	F-H388R	F (coat) -D_1 (external scaffolding) contact site
			G3158A	H-M76I	
φX WT ev-o2	12.9 ± 0.3	WT φX	C1470T	F-D154E	F-D_1 contact site
			G2120A	F-E373K	F-D_1 contact site
			A3055G	H-K53E	
CNVA	ND	χ2	C367T	C-Q79och	Decreases expression of all viral genes[e]
			A1464G	F-D154G	F-D_1 contact site
			C2280T	F-S426L	Known suppressor of defective D protein function[f]
χ2 V anc.	7.8 ± 0.5	χ2	A2276G	F-T425A	Known suppressor of defective D protein function[f]
			G2371C		F-G intercistronic region – increased G protein levels[e]
			G2379A		F-G intercistronic region – increased G protein levels[e]
χ2 V ev-o1	13.1 ± 0.5	χ2	G2179T	F-Q392H	F-G contact site
			G3111A	H-V61I	
χ2 V ev-o2	14.1 ± 0.2	χ2	G2000A	F-V333I	F-D_4 contact site
			G2179T	F-Q392H	F-G contact site
			G3039T	H-V37L	
G4GV anc.	7.3 ± 0.4	WT G4	C367T	C-Q79och	Decreases expression of all viral genes[e]
			A1464G	F-D154G	F-D_1 contact site
			C2280T	F-S426L	Known suppressor of defective D protein function[f]
G4GV ev-o1	11.6 ± 0.3	WT G4	G2179T	F-Q392H	F-G contact site
			G2379A		F-G intercistronic region – increased G protein levels[e]
			A3340G	H-D137G	

(continued on next page)

Table 1 *(continued)*

Strain	Fitness[a]	G protein[b]	Genotypic changes[c]: Nucleotide	Amino acid	Hypothesized Function and/or structural contacts[d]
G4GV evo2	12.9 ± 0.4	WT G4	G2379A		F-G intercistronic region – increased G protein levels[e]
			G2387T		F-G intercistronic region – increased G protein levels[e]
			A3055G	H-N42S	
			A3109G	H-N60S	

[a] Fitness is expressed as doublings per hour with standard deviation, n =3.

[b] Indicates that G (spike) gene and protein found in the strain. The χ2 gene and protein is 94% G4 and 6% φX174 in origin. See text for details.

[c] Nucleotide changes are denoted with the original base followed by the nucleotide in the published sequence (Sanger et al., 1978). Thus, G3039T indicates a G→T substitution at position 3039 T. For amino acid changes, the letter before the hyphen indicates the gene and protein: F (coat), G (spike) and H (DNA pilot). The original amino acid precedes the amino acid number position in the protein, which is followed by the substitution. Thus, F-Q392H indicates a Q→H substitution at amino acid 392 in the coat protein.

[d] structural contacts were taken from the x-ray structures of the φX174 virion and procapsid (Dokland et al., 1999; Dokland et al., 1997; McKenna et al., 1996; McKenna et al., 1994).

[e] reference (Doore and Fane, 2015).

[f] references (Cherwa and Fane, 2009; Cherwa et al., 2008; Uchiyama et al., 2007).

assembly, the φXG4G chimera may have been presented with a tradeoff between efficient attachment and morphogenesis. However, without morphogenesis, no particles would exist to initiate a subsequent infection: thus, particle assembly was likely the primary target of selection.

2.2. Experimental evolution of chimeric viruses yields higher-fitness variants

To examine how the φXG4G chimeras could recover fitness, the viable strains were experimentally evolved. Initially, χ^2V and G4GV were serially passaged in liquid culture, which is the preferred method for experimentally evolving microviruses (Wichman and Brown, 2010). However, both strains repeatedly died out before the tenth passage, despite varying the incubation time, multiplicity of infection (MOI) and bottleneck size. As an alternative approach, two single plaques were picked from each ancestral strain and independently propagated by stabbing phage onto plates. Plates were incubated overnight at 33 °C, providing ample time for clearings to form. To circumvent complications associated with spatial structure (Ally et al., 2014), samples were collected from multiple locations throughout the clearing for each successive transfer. As a control, two wild-type φX174 plaques were subjected to the same protocol. By the end of 15 serial passages, plaques were re-isolated, sequenced, and characterized. As shown in Table 1, all evolved chimera strains had higher fitness than their respective ancestors, whereas evolved wild-type strains exhibited no significant fitness differences. Evolved strains are denoted "evo1" or "evo2" according to the plaque from which they were started. Plaques area was also measured. Approximately one hundred plaques from each strain were evaluated. Although there was a trend toward larger plaques for the evolved χ^2V and G4GV strains, naturally occurring size variations created large deviations in area and error, proving to be a less reliable measure of fitness (data not shown).

The additional mutations found in the evolved strain are listed in Table 1. No previously acquired mutations were lost. Mutations altering coat-external scaffolding protein contact sites and the DNA pilot protein H arose in all evolved strains, including wild-type. Mutations in gene H are commonly observed during experimental evolution in chemostats at high viral densities (Bull et al., 1997; Crill et al., 2000; Pepin et al., 2008; Wichman et al., 2000), which would also occur in plaques. Thus, these mutations may have arisen due to the propagation method and may generally elevate fitness under high-density conditions. The strains evolved from wild-type did not display a significantly elevated fitness compared to their ancestor: however, since wild-type is already reasonably fit, small increases may be more difficult to detect. Here, and in the previous study (Doore and Fane, 2015), it was very difficult to obtain reasonably pure high titer stocks. Additional mutations often swept through the population during stock growth. Thus, separating the multiple mutations occurring in the evolved strains to individually assess each one's respective contribution to fitness was problematic. In addition, epistasis has been well-documented in microvirus genomes (Caudle et al., 2014; Pearson et al., 2012; Rokyta et al., 2011). Thus, mutations that arose during serial passages may not necessarily have measurable fitness effects alone.

In contrast to the ubiquitous H gene mutations, the mutations altering the F-G intercistronic region and the coat-major spike protein interface arose only in the evolved chimeric strains. The ancestral χ^2V strain began with two mutations in the intercistronic region, which presumably results in increased intracellular concentrations of the major spike protein (Doore and Fane, 2015). In the previous study and with one of the mutants herein (see Table 3), increasing mutant protein levels by concurrently expressing the mutant gene from a plasmid and the genome rescued plaque formation. However, in whole cell lysates, it was difficult to accurately detect differences between strains with and without the intercistronic mutations. The difference may be too slight to discern or the changes reflect a more complex undefined mechanism, which cannot be excluded. The ancestral G4GV strain began with no changes in the F-G intercistronic region: however, the evolved strains acquired mutations at or near those found in the ancestral χ^2V strain. The G4GV evo2 strain acquired two intercistronic substitutions; G4GV evo1 acquired one, along with a mutation at the coat-major spike protein interface, F-Q392H (glutamine → histidine at residue 392 in the coat protein F). Both evolved χ^2V strains acquired the F-Q392H substitution. Sequencing earlier populations indicated that these mutations appeared before substitutions in gene H, suggesting that increased major spike protein concentration and/or altered coat-major spike protein interactions were the primary selective targets in the chimeric backgrounds.

2.3. Mutations in the evolved chimeric strains restore assembly kinetics but their effect on attachment kinetics is unclear

As described above, attachment and assembly kinetics were determined for the evolved chimera strains (Fig. 3C–F). Neither evolved wild-type strain differed significantly from their ancestor in these assay (data not shown). The restoration of attachment kinetics was defined here as statistical significance between the ancestral and evolved strain at both the 3 and 6 min time points, as expressed by non-overlapping error bars. By this stringent criterion, the mutations in the evolved strains do not elevate attachment efficiency over that observed for the ancestors. By contrast, the mutations in the evolved strains have a more dramatic effect on assembly kinetics. As shown in Fig. 3D, the lag phase of the evolved χ^2V strains was reduced by 5–10 min, with the greatest increase in progeny production between 20 and 25 min post infection. This corresponds with the approximate doubling and lysis time of the host. Similarly, the evolved G4GV strains maintained ancestral assembly kinetics, but the *magnitude* of particle production was increased (Fig. 3F). Since the assembly kinetics of the ancestral G4GV strain is not as severely affected as χ^2V, simply elevating the

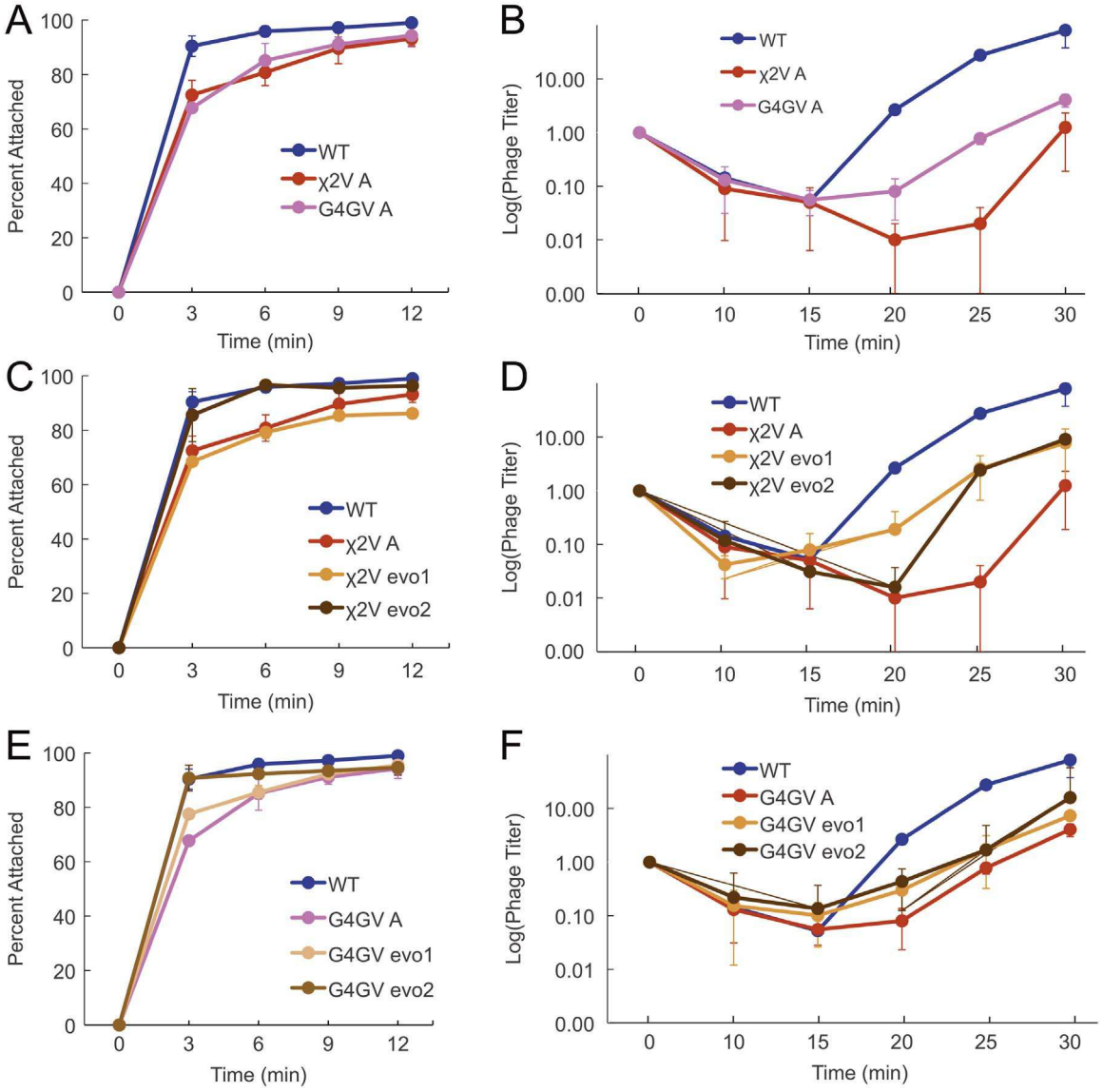

Fig. 3. Attachment (A, C, and E) and assembly kinetics (B, D, and F) of wild-type and chimeric particles. Each graph represent the averages of three assays with standard deviation. A) Attachment kinetics of wild-type and ancestral chimeras. B) Assembly kinetics of wild-type and ancestral chimeras. C) Attachment kinetics of wild-type, ancestral χ^2V, and evolved χ^2V strains. D) Assembly kinetics of wild-type, ancestral χ^2V, and evolved χ^2V strains. E) Attachment kinetics of wild-type, ancestral G4V, and evolved G4V strains. F) Assembly kinetics of wild-type, ancestral G4V, and evolved G4V strains.

amount of particles produced may have been more beneficial in this context. In both cases, cells infected with the evolved strains would produce more progeny prior to lysis.

2.4. The chimeric χ^2 major spike G protein does not participate in assembly as efficiently as either wild-type protein

The χ^2V and G4GV strains had a common non-viable ancestor (CNVA: see Table 1 for genotype) that encodes the chimeric χ^2V G protein. Two observations suggest that chimeric χ^2V G protein was less efficiently incorporated into virions than either the wild-type φX174 and G4 proteins. First, exogenous expression of the wild-type φX174 or G4 major spike gene rescued CNVA; however, rescue was not observed when the chimeric major spike gene was similarly expressed (Doore and Fane, 2015). Second, replacing the chimeric G gene with the G4 G gene yielded the viable G4GV strain, whereas the viable χ^2V needed additional mutations to reach viability (Doore and Fane, 2015). To test this hypothesis, chimeric viruses were assembled in cells expressing a cloned, HA-tagged version of the wild-type φX174 protein (φX174G-HA, hereafter referred to as G-HA). This tag enables the differentiation between genome-derived and plasmid-derived G proteins via SDS-PAGE. Induction of the cloned gene rescues *am(G)* mutants and does not inhibit wild-type plaque formation (Christakos et al., 2015).

After purification by rate zonal sedimentation, the composition of assembled particles was analyzed by SDS-PAGE and densitometry. Ratios of genome-derived (G) versus plasmid-derived (G-HA) were calculated to determine the G protein "preference" in virions. The virion fractions for all strains are shown in Fig. 4. Wild-type φX174 virions contained approximately equal amounts of both G proteins, suggesting no significant incorporation differences between the wild-type φX174 and HA-tagged proteins. There was no detectable genome-derived chimeric G proteins found in assembled CNVA particles, which contained only the HA-tagged φX174 protein. This indicates that the G protein encoded by CNVA, which is derived from G4 but contains 5 non-conserved C-terminal amino acids from φX174, is unable to compete with the wild-type derived HA-tagged protein.

Although a viable strain encoding the chimeric protein was isolated, the ancestral χ^2V strain, it contains three mutations not found in CNVA. Two of these are point mutations in the F-G intercistronic region, which regulates G gene expression. Unlike CNVA particles, χ^2V

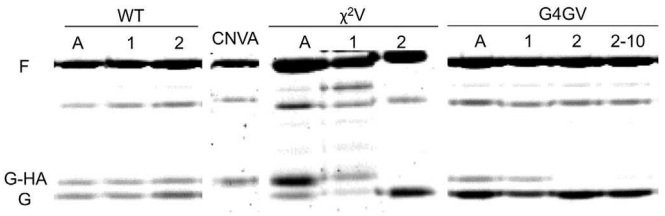

Fig. 4. SDS-PAGE of virions assembled in cells expressing the tagged φX174 major spike G gene (G-HA). The χ^2V A and χ^2V evo1 particles appeared to be unstable during purification. Thus, the final samples had to be concentrated before electrophoresis and silver staining had to be employed, which likely accounts for the higher level of host cell proteins in the sample. χ^2V evo2 particles were also silver stained but not concentrated. Wild-type, CNVA, and G4GV, ancestral and evolved virions were coomassie stained. Abbreviations: A, ancestor; CNVA, common non-viable ancestor. Numbers represent evo1 and evo2 of the chimeric strains. The G4GV evo2 strain isolated after the 10th passage, which does not contain mutations in gene H, is designated 2–10.

particles contained a mix of G proteins. This is likely caused by increased expression of the genome-encoded chimeric gene. The virions of the ancestral G4GV strain, which differs from CNVA by encoding the full-length G4 major spike gene, contained more genome-derived G4 major spike proteins than plasmid-encoded, HA-tagged φX174 protein. The G4G: G-HA protein ratio appeared to be greater than that found in the wild-type φX174 control. This suggests that the foreign, wild-type major spike protein may be slightly "preferred" in the G4GV background.

To determine whether further adaptation affected particle composition, the evolved strains were examined by the same assay. As expected, neither wild-type evolved strain differed significantly from their ancestor (Fig. 4). Although similar results were obtained for the χ^2V evo1 strain and its respective ancestor, the evo2 strain appeared to incorporate exclusively genome-derived G proteins. Both evolved strains contain F-Q392H mutation at the coat-major spike interface. However, χ^2V evo2 strain also contains a mutation near a coat-external scaffolding protein (subunit 4) contact site, F-V333I. This change could be altering the external scaffolding protein lattice, allowing it to accommodate chimeric 12 S* particles over wild-type 12 S* particles during procapsid formation. The χ^2V A and χ^2V evo1 particles appeared to be unstable during purification. Thus, the final samples had to be concentrated before electrophoresis and silver staining had to be employed, which likely accounts for the higher level of host cell proteins in the sample. Coomassie blue staining was adequate to visualize the proteins in all other samples.

As with the evolved χ^2V strains, the evolved G4GV strains displayed different relative ratios of G protein incorporation: the G protein composition of the evo1 strain was similar to the ancestor, whereas the evo2 strain exclusively incorporated the genome-derived G4 G protein. The evo2 strain acquired two mutations in the F-G intercistronic region, likely elevating the expression of the G4 G gene. This strain also contains two mutations in gene H. As described above, mutations in gene H commonly arise during experimental evolution when phage populations are maintained at high density. Consistent with this observation, the H mutations in G4GV evo2 arose after multiple passages at high density, between generations 10 and 11. However, to exclude the possibility that these mutations affect major spike protein preference, we examined the composition of generation 10 virions assembled in the presence of G-HA. As shown in the rightmost lane of Fig. 4, evo2-gen10 still contains primarily genome-derived G. Thus, the altered particle composition of G4GV evo2 is likely due to an increase in concentration of the genome-encoded major spike protein, rather than structural changes in the coat protein as observed in the χ^2V evo2 lineage.

Table 2
Efficiency of plating[a] of wild-type and φXG4GC-term mutants at various temperatures.

Genotype[b]	Temperature			Hypothesized function and/or structural contacts[c]
	22 °C	33 °C	42 °C	
Wild-type	1.0	1.0	1.0	
φXG4GC-term	10^{-5}	1.0	1.0	
φXG4GC-term/F-S1F	1.0	1.0	0.6	Suppressor of defective packaging[d]
φXG4GC-term/F-G88V	1.0	1.0	0.1	Suppressor of defective packaging[e]
φXG4GC-term/F-D154N	0.5	1.0	1.0	F-D_1 contact[c]
φXG4GC-term/F-Y210H	0.6	1.0	0.6	Possible suppressor of defective D protein function[f]
φXG4GC-term/F-V318F	1.0	0.6	0.5	F-D_4 contact
φXG4GC-term/F-L319F	0.4	1.0	0.2	F-D_4 contact
φXG4GC-term/F-H388R	0.6	1.0	0.9	F-D_1 contact
φXG4GC-term/F-T425I	1.0	0.8	0.6	
φXG4GC-term/G-A106V	1.0	0.2	1.0	G-D_1 contact, suppressor of defective D protein function[g]
φXG4GC-term/G-P136S	0.5	1.0	0.5	Near F-G interface, G-D_1 contact
φXG4GC-term/G-P136T	1.0	1.0	0.4	Near F-G interface, G-D_1 contact

[a] Efficiency of plating is defined as the assay titer/titer at 33 °C.
[b] Suppressors of the cold-sensitive *φXG4GC-term* phenotype are listed after the dash (/). Names reflect alterations on the protein level. The letter before the hyphen indicates the altered gene and protein: F (coat) and G (spike) and H (DNA pilot). The original amino acid precedes the amino acid position in the protein, which is followed by the substitution. Thus, G-P136T indicates a P→T substitution at amino acid 136 in the spike protein.
[c] Structural contacts were taken from the x-ray structures of the φX174 virion and procapsid (Dokland et al., 1999; Dokland et al., 1997; McKenna et al., 1996; McKenna et al., 1994).
[d] References (Hafenstein and Fane, 2002; Hafenstein et al., 2004; Jennings and Fane, 1997).
[e] Reference (Ekechukwu et al., 1995).
[f] Amino acid 210 resides in an α-helix in which numerous suppressors of D defective D protein function have been isolated (Cherwa and Fane, 2009; Cherwa et al., 2008; Fane et al., 1993; Uchiyama et al., 2007; Uchiyama and Fane, 2005).
[g] Reference (Uchiyama et al., 2007).

2.5. A "reverse χ^2" gene in the φX174 background was generated to create the φXG4GC-term mutant

In the previous study, it was also hypothesized that the C-terminal end of G4 was responsible for raising a thermodynamic and/or kinetic barrier to φX174 assembly (Doore and Fane, 2015). By recombining out the C-terminal end to produce φXG4G/χ^2, this barrier was minimized. To investigate the assembly barrier conferred by this specific region, the C-terminal encoding end of the G4 major spike G gene was engineered into an otherwise wild-type φX174 background (Fig. 1). The resulting φXG4GC-term mutant was viable above 24 °C but exhibited a cold-sensitive (*cs*) phenotype. Plaques became small and turbid at 24 °C and no longer formed at 22 °C (Table 2). As was done for the initial characterization of the chimeric strains, attachment and eclipse kinetics of the φXG4GC-term mutant were assayed at the restrictive temperature. Neither attachment nor eclipse differed significantly from wild-type (data not shown). Thus, potential assembly defects contributing to the *cs* phenotype were investigated.

2.6. The φXG4GC-term mutant has multiple morphogenetic defects

To examine particle formation of this mutant, assembly intermediates were allowed to accumulate in lysis-resistant cells at the restrictive

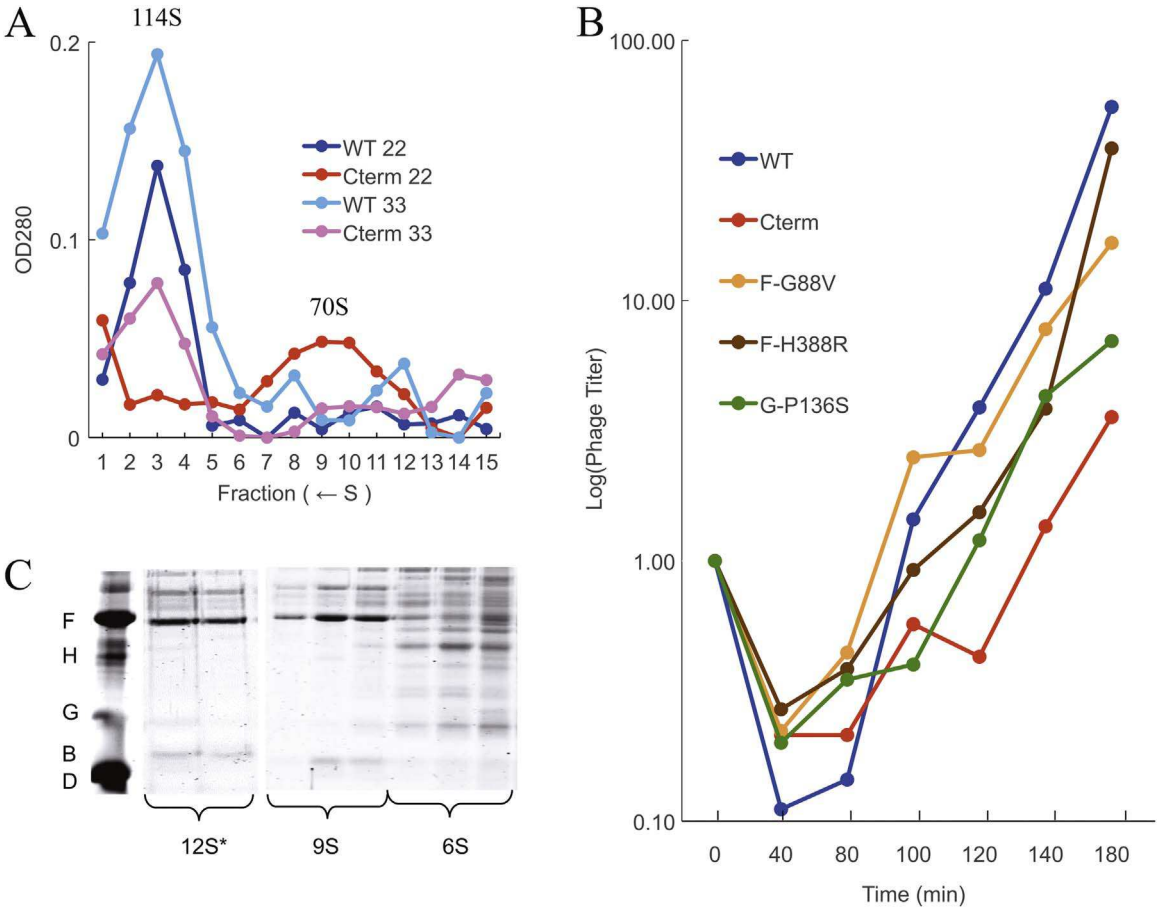

Fig. 5. Characterization of φXG4GC-term assembly. A) Sedimentation profiles of φXG4GC-term large particles under permissive (33 °C) and restrictive (22 °C) conditions compared to wild-type. The position of virions (114 S) and degraded procapsids (70 S) are indicated on the graph. B) Assembly kinetics of wild-type, φXG4GC-term, and second-site suppressors at 22 °C. C) Small particle composition of φXG4GC-term infected cell extracts. Different ultracentrifuge parameters are required to examine the large particles (S > 70 S) and small assembly intermediates (S≤12 S). Thus, the fractions examined by SDS-PAGE differ from those in panel A. Proteins were stained with coomassie blue.

or permissive temperature, 22 °C or 33 °C respectively. Following chemical lysis of infected cells, intermediates were separated by rate-zonal sedimentation. Large particles, comprised of virions (114 S) and degraded procapsids (70 S), are shown in Fig. 5A. At the permissive temperature, primarily virions were produced from the wild-type and mutant infections, with relatively few degraded procapsids. Both particles were equally infectious, with specific infectivities of 1×10^{12} pfu (plaque forming units)/A_{280} at the peak fraction. At 22 °C, the wild-type large particle profile and virion specific infectivity remained the same. However, the φXG4GC-term profile was significantly altered, with the largest peak corresponding to 70 S degraded procapsids, potentially indicative of DNA packaging defects (Burch and Fane, 2000; Cherwa and Fane, 2009; Cherwa et al., 2008; Uchiyama et al., 2007; Uchiyama and Fane, 2005). Although a distinct peak was not visible, some mutant particles did sediment at 114 S. However, their specific infectivity is 7×10^{10} pfu/A_{280}, representing a significant reduction compared to wild-type and permissively-produced mutant particles.

The low levels of infectious virions as well as 70 S φXG4GC-term particles were produced in lysis resistant cells incubated for 5 h. This suggests that assembly intermediates can interact, albeit inefficiently, and may require higher critical concentrations of intermediates for assembly to occur. To test this hypothesis, assembly kinetics were investigated at the restrictive temperature. Similar to the aforementioned chimeric strains, the kinetics of particle formation was significantly delayed (Fig. 5C). At 22 °C, wild-type particle formation shows a steep increase between 80 and 100 min. By contrast, the C-term mutant only shows a modest increase between 120 and 140 min. The doubling time of the host at this temperature was approximately 110 min. In lysis-resistant cells, some particles would be able to form after 5 h (300 min), which is consistent with the observed low level of particles described above. However, in lysis-sensitive cells, programmed cell lysis would preclude progeny production. The wild-type and φXG4GC-term mutant experiments were performed twice. In both instances wild-type yields, wild-type yields steeply rose 40 min earlier than the mutant. During the second experiment, the second-site suppressors strains were examined in concert.

To examine possible early assembly defects, small particles, consisting of early assembly intermediates, were analyzed. As is typical, no excess intermediates were detected in wild-type infected cell extracts (data not shown): all had assembled into large particles. Conversely, 6 S and 9 S* particles were detected within the φXG4GC-term mutant-infected cell extracts, with a minor accumulation of 12 S* particles (Fig. 5B). However, levels of these intermediates were still low, and no particle accumulated to gross excess, which is typically observed when a mutation affects only one morphogenetic step (Cherwa et al., 2008; Gordon and Fane, 2013; Gordon et al., 2012). Results from these analyses suggest that multiple blocks in the assembly pathway contribute to the *cs* phenotype.

2.7. The φXG4GC-term mutant could be rescued by over-expression of the wild-type external scaffolding D or the φXG4GC-term G gene

To test hypotheses regarding the multiple assembly defects, rescue experiments were performed using cloned viral genes (Table 3). The φXG4GC-term phage were plated on cells over-expressing a cloned

Table 3
Efficiency of plating[a] of wild-type and φXG4GC-term mutants on cells expressing cloned viral genes.

	Expressed cloned gene:							
	None		φXB		φXD		φXG4GC-term	
Genotype	22 °C	33 °C	22 °C	33 °C	22 °C	33 °C	22 °C	33 °C
Wild-type φX174	1.0	1.0	1.0	1.0	1.0	1.0	1.0	1.0
φXG4GC-term	10^{-5}	1.0	10^{-5}	1.0	0.3	1.0	0.1	1.0

[a] Plating efficiency is defined as assay titer/most permissive titer.

gene encoding the φXG4GC-term protein G, the external scaffolding protein D, or the internal scaffolding protein B. Rescue was defined as the ability for plaques to form above 10^{-5}, the previously determined plating efficiency at 22 °C. Over expression of either the φXG4GC-term major spike G or the external scaffolding D gene rescued the φXG4GC-term mutant. If the 9 S*+ 6 S → 12 S* transition is inefficient (Fig. 1A), increasing the intracellular 6 S particle concentration by exogenous φXG4GC-term gene could drive this reaction forward. This would result in a greater 12 S* particle concentrations. Elevating levels of either the 12 S* particles or the external scaffolding protein D via exogenous D gene expression could drive an inefficient 12 S*→ procapsid transition. By contrast, the internal scaffolding protein binds coat protein pentamers prior to the 9 S*+ 6 S → 12 S* and 12 S*→ procapsid transitions: thus, it should not be affected by G protein mutations. Consistent with this hypothesis, rescue by exogenous internal scaffolding B gene expression was not observed.

2.8. Second-site suppressors of the cs phenotype restore assembly of the φXG4GC-term mutant

To determine how the inefficient protein-protein interactions in φXG4GC-term could be corrected, second-site suppressor strains were isolated at the restrictive temperature. These arose at a frequency of 10^{-6} and are listed in Table 2. Substituted amino acids mapped primarily to coat-external scaffolding protein contact sites, the coat-spike protein interface, and/or sites known to correct packaging defects. Three second-site suppressors were assayed for assembly kinetics. These experiments were performed twice. However, different suppressors were analyzed with the controls in different experiments. All suppressors had reduced lag phases prior to progeny production (Fig. 5C). F-G88V and F-H388R were strong suppressors, reducing the lag phase by approximately 40 min and resembling wild-type kinetics. The G-P136S suppressor was weaker, only modestly reducing the lag phase by 20 min. However, in both cases, progeny would still be produced prior to cell lysis at 110 min

2.9. Summary

All chimeric strains described herein displayed at least one defect during the infection cycle. For the χ^2V and G4GV strains, which encode primarily the G4 major spike gene, these defects manifested as delayed attachment and assembly kinetics. For the φXG4GC-term strain, which encodes only the C-terminus of the G4 major spike gene, these defects affected assembly kinetics only. In all cases, suppression of these defects involved multiple possible mechanisms, including the alteration of protein-protein interactions and/or putative changes in gene expression.

In Doore and Fane (2015), the original φXG4G chimera had to overcome multiple thermodynamic and kinetic barriers to assembly. The foreign protein promoted non-productive, off-pathway reactions over productive ones. These non-productive interactions were initially suppressed by a global reduction in foreign gene expression. Productive reactions could then be modified while the inhibitory protein was produced at lower concentrations. Once productive reactions were modified, gene expression could be re-elevated to force inefficient assembly reactions forward. Viability was ultimately attained after further increases in expression of the chimeric χ^2 major spike gene, producing χ^2V; or after a recombination event placing the full-length G4 major spike gene in the genome, producing G4GV. Though viable, these chimeras exhibited reduced fitness, suggesting some thermodynamic and/or kinetic barrier still existed. During experimental evolution, this lower barrier could be overcome by similar mechanisms leading to initial chimera viability. Additional structural changes and/or further increases in protein levels restored fitness to near wild-type levels. Although we hypothesize that the changes in the F-G intercistronic region are increasing the intracellular levels of the G protein, it was difficult to accurately detect differences between strains with and without the intercistronic mutations. The difference may be too slight to discern or the changes reflect a more complex undefined mechanism, which cannot be excluded. For the φXG4GC-term mutant, these mechanisms were also employed to overcome inefficient assembly. This mutant could be rescued by increasing protein concentrations, as was done by inducing cloned genes on plasmids; or by direct structural changes, as was seen with second-site suppressors.

3. Materials and methods

3.1. Phage plating, media, buffers, and stock preparation

Media, buffers, plating and liquid culture stock preparations have been previously described (Fane and Hayashi, 1991).

3.2. Bacterial strains, plasmids and φX174 mutants

The *Escherichia coli* C strain BTCC 122 (C122) has been previously described (Fane and Hayashi, 1991). BAF30 is a *recA*- derivative of C122 (Fane et al., 1992). The RY7211 cell line contains a mutation in the *mraY* gene rendering it resistant to E protein-mediated lysis (Bernhardt et al., 2000, 2001). Clones of the viral genes φXB (Novak and Fane, 2004), φXD (Cherwa et al., 2008), φXG-HA (Christakos et al., 2015) φXG and G4G (Doore and Fane, 2015) have been previously described. The clone of the mutant φXG gene containing the conserved amino acid residues found in the G4 G protein (pφXG4GC-term) was obtained as previously described (Doore and Fane, 2015). However, the downstream primer introduced the five G4 codons that encode amino acids that differ between the two sequences. The φXG4GC-term mutant was generated via site directed mutagenesis as previously described (Fane et al., 1993) using a mutagenic primer that introduced the five G4 codons mentioned above. The primer was designed to anneal to the positive strand (5′-CTCACTTAAGTGGCTGGAGAACAGTAGCCTCTCTATTAACCTGATTC-AGC-3′).

3.3. Serial passages of viable chimeras

Experimental evolution of microvirus strains typically occurs in liquid culture (Ally et al., 2014; Bull et al., 1997; Wichman et al., 1999). However, both strains were repeatedly lost before 10 passages despite varying the multiplicity of infection (MOI) from 0.01 −1.0 and/or the incubation times from 30 to 90 min. Therefore an alternate methodology was employed. Two single plaques from wild-type, χ^2V, and G4GV each were picked and stabbed into plates seeded with C122 and subsequently passaged in parallel. The chimeras formed very small plaques: thus, plates were allowed to incubate at 33 °C for at least 10 h before the next passage. To transfer phage to a new plate, one toothpick was used to stab one clearing multiple times and then stabbed once into the new plate. Stabs were separated by at least 5 cm to reduce the risk of cross-contamination. This process was repeated 15 times. After

the final passage, single plaques were isolated for sequencing and growing stocks.

Attachment, eclipse and fitness assays: Fitness assays and fitness calculations were performed as previously described (Bull et al., 1997). Attachment assays were performed as previously described (Hafenstein et al., 2004). Briefly, lysis resistant cells were grown to a concentration of 1.0×10^8 cells/ml and concentrated 5-fold in growth media (1.0% tryptone, 0.5% KCL). $MgCl_2$ and $CaCl_2$ were added to a concentration of 10 mM and 5.0 mM, respectively. Approximately 1.0×10^6 phage were added to 1.0 ml of cells and incubated at 37^0 C for specified time intervals (see figures). At sampling times, attached phage were removed by centrifugation. Supernatants were titered to determine the level of unattached virions. Attachment and eclipse assays were performed as previously described (Cherwa et al., 2009; Hafenstein et al., 2004), but with pre-attachment at 16 °C for 30 min prior to eclipse. Briefly, exponential lysis resistant cells were concentrated and resuspended in HFB buffer [0.06 M NH_4Cl, 0.09 M NaCl, 0.1 M KCl, 0.1 M Tris-HCl (pH 7.4),1.0 mM $MgSO_4$,1.0 mM $CaCl_2$] with 10 mM $MgCl_2$ and 0.5 mM $CaCl_2$. After infection, samples were incubated at 16 °C for 30 min. Unattached virions were removed by centrifugation. The cell pellets with attached phage were resuspended in 1.0 ml ice-cold HFB with 10 mM $MgCl_2$ and 0.5 mM $CaCl_2$ and placed into a 37 °C water bath to initiate the eclipse reaction. At selected time points, samples were diluted 1/10 in Borate-EDTA buffer (50 mM $Na_2B_4O_7$, 3.0 mM EDTA), which releases un-eclipsed phages from cell membranes, and titered for surviving particles.

3.4. In vivo *characterization of assembly intermediates and kinetics*

Protocols for generating extracts of infected lysis-resistant cells, ultracentrifugation parameters, and particle detection have been previously described (Uchiyama et al., 2007; Uchiyama and Fane, 2005). Briefly, 100 ml of exponentially growing lysis resistant cells ($1–2\times10^8$) were infected at a multiplicity of infection (MOI) of 3.0. Cells were pelleted and resuspended in sucrose gradient buffer [100 mM NaCl, 5.0 mM ethylenediaminetetraacetic acid (EDTA), 6.4 mM Na2HPO4 and 3.3 mM KH2PO4 (pH 7.0)] and lysed with lysozyme (2.0 mg/ml). Extracts were concentrated to 200 µl and layered atop 5–30% sucrose gradients, then spun at 45,000 rpm for 1 h in a SW50.1 rotor. Gradients were divided into 100 µl fractions by dripping from the bottom of the tube. Material was detected by taking OD_{280} readings of each fraction. The position of infectious virion was determined by titering. To examine small assembly intermediates, gradients were spun at 34,000 rpm and fractions were analyzed by SDS-PAGE. The protocol to examine in vivo kinetics has been previously described (Uchiyama et al., 2007; Uchiyama and Fane, 2005). Briefly, mid-exponential lysis-resistant cells were infected at an MOI of 0.01. For each time point, 100 µl of sample was removed and diluted 1:10 with BE (50 mM $Na_2B_4O_7$, 3.0 mM EDTA) containing 2.0 mg/ml hen egg white lysozyme to release assembly intermediates. Fully-assembled, infectious progeny were quantified by plaque assays.

Acknowledgements

The authors acknowledge the support of the National Science Foundation (MCB1408217 to B.A.F).

References

Ally, D., Wiss, V.R., Deckert, G.E., Green, D., Roychoudhury, P., Wichman, H.A., Brown, C.J., Krone, S.M., 2014. The impact of spatial structure on viral genomic diversity generated during adaptation to thermal stress. PLoS One 9, e88702.
Bernal, R.A., Hafenstein, S., Olson, N.H., Bowman, V.D., Chipman, P.R., Baker, T.S., Fane, B.A., Rossmann, M.G., 2003. Structural studies of bacteriophage alpha3 assembly. J. Mol. Biol. 325, 11–24.
Bernhardt, T.G., Roof, W.D., Young, R., 2000. Genetic evidence that the bacteriophage phi X174 lysis protein inhibits cell wall synthesis. Proc. Natl. Acad. Sci. USA 97, 4297–4302.
Bernhardt, T.G., Struck, D.K., Young, R., 2001. The lysis protein E of phi X174 is a specific inhibitor of the MraY-catalyzed step in peptidoglycan synthesis. J. Biol. Chem. 276, 6093–6097.
Bull, J.J., Badgett, M.R., Wichman, H.A., Huelsenbeck, J.P., Hillis, D.M., Gulati, A., Ho, C., Molineux, I.J., 1997. Exceptional convergent evolution in a virus. Genetics 147, 1497–1507..
Burch, A.D., Fane, B.A., 2000. Foreign and chimeric external scaffolding proteins as inhibitors of Microviridae morphogenesis. J. Virol. 74, 9347–9352.
Burch, C.L., Chao, L., 1999. Evolution by small steps and rugged landscapes in the RNA virus phi6. Genetics 151, 921–927.
Caudle, S.B., Miller, C.R., Rokyta, D.R., 2014. Environment determines epistatic patterns for a ssDNA virus. Genetics 196, 267–279.
Cecchini, N., Schmerer, M., Molineux, I.J., Springman, R., Bull, J.J., 2013. Evolutionarily stable attenuation by genome rearrangement in a virus. G3 (Bethesda) 3, 1389–1397.
Cherwa, J.E., Jr., Fane, B.A., 2009. Complete virion assembly with scaffolding proteins altered in the ability to perform a critical conformational switch. J. Virol. 83, 7391–7396.
Cherwa, J.E., Jr., Organtini, L.J., Ashley, R.E., Hafenstein, S.L., Fane, B.A., 2011. In vitro assembly of the σX174 procapsid from external scaffolding protein oligomers and early pentameric assembly intermediates. J. Mol. Biol. 412, 387–396.
Cherwa, J.E., Jr., Sanchez-Soria, P., Wichman, H.A., Fane, B.A., 2009. Viral adaptation to an antiviral protein enhances the fitness level to above that of the uninhibited wild type. J. Virol. 83, 11746–11750.
Cherwa, J.E., Jr., Uchiyama, A., Fane, B.A., 2008. Scaffolding proteins altered in the ability to perform a conformational switch confer dominant lethal assembly defects. J. Virol. 82, 5774–5780.
Christakos, K.J., Chapman, J.A., Fane, B.A., Campos, S.K., 2015. PhiXing-it, displaying foreign peptides on bacteriophage PhiX174. Virology 488, 242–248.
Crill, W.D., Wichman, H.A., Bull, J.J., 2000. Evolutionary reversals during viral adaptation to alternating hosts. Genetics 154, 27–37.
Diemer, G.S., Stedman, K.M., 2012. A novel virus genome discovered in an extreme environment suggests recombination between unrelated groups of RNA and DNA viruses. Biol. Direct 7, 13.
Dokland, T., Bernal, R.A., Burch, A., Pletnev, S., Fane, B.A., Rossmann, M.G., 1999. The role of scaffolding proteins in the assembly of the small, single-stranded DNA virus phiX174. J. Mol. Biol. 288, 595–608.
Dokland, T., McKenna, R., Ilag, L.L., Bowman, B.R., Incardona, N.L., Fane, B.A., Rossmann, M.G., 1997. Structure of a viral procapsid with molecular scaffolding. Nature 389, 308–313.
Doore, S.M., Fane, B.A., 2015. The kinetic and thermodynamic aftermath of horizontal gene transfer governs evolutionary recovery. Mol. Biol. Evol. 32, 2571–2584.
Doore, S.M., Fane, B.A., 2016. The microviridae: diversity, assembly, and experimental evolution. Virology 491, 45–55..
Ekechukwu, M.C., Oberste, D.J., Fane, B.A., 1995. Host and phi X 174 mutations affecting the morphogenesis or stabilization of the 50S complex, a single-stranded DNA synthesizing intermediate. Genetics 140, 1167–1174.
Fane, B.A., Hayashi, M., 1991. Second-site suppressors of a cold-sensitive prohead accessory protein of bacteriophage phi X174. Genetics 128, 663–671.
Fane, B.A., Head, S., Hayashi, M., 1992. Functional relationship between the J proteins of bacteriophages phi X174 and G4 during phage morphogenesis. J. Bacteriol. 174, 2717–2719..
Fane, B.A., Shien, S., Hayashi, M., 1993. Second-site suppressors of a cold-sensitive external scaffolding protein of bacteriophage phi X174. Genetics 134, 1003–1011..
Froissart, R., Wilke, C.O., Montville, R., Remold, S.K., Chao, L., Turner, P.E., 2004. Co-infection weakens selection against epistatic mutations in RNA viruses. Genetics 168, 9–19.
Gibbs, M.J., Weiller, G.F., 1999. Evidence that a plant virus switched hosts to infect a vertebrate and then recombined with a vertebrate-infecting virus. Proc. Natl. Acad. Sci. USA 96, 8022–8027.
Gordon, E.B., Fane, B.A., 2013. The effects of an early conformational switch defect during øX174 morphogenesis are belatedly manifested late in the assembly pathway. J. Virol. 87, 2518–2525.
Gordon, E.B., Knuff, C.J., Fane, B.A., 2012. Conformational Switch-Defective øX174 Internal Scaffolding Proteins Kinetically Trap Assembly Intermediates before Procapsid Formation. J. Virol. 86, 9911–9918.
Hafenstein, S., Fane, B.A., 2002. Phi X174 genome-capsid interactions influence the biophysical properties of the virion: evidence for a scaffolding-like function for the genome during the final stages of morphogenesis. J. Virol. 76, 5350–5356.
Hafenstein, S.L., Chen, M., Fane, B.A., 2004. Genetic and functional analyses of the σX174 DNA binding protein: the effects of substitutions for amino acid residues that spatially organize the two DNA binding domains. Virology 318, 204–213..
Hendrix, R.W., Smith, M.C., Burns, R.N., Ford, M.E., Hatfull, G.F., 1999. Evolutionary relationships among diverse bacteriophages and prophages: all the world's a phage. Proc. Natl. Acad. Sci. USA 96, 2192–2197.
Jennings, B., Fane, B.A., 1997. Genetic analysis of the phi X174 DNA binding protein. Virology 227, 370–377.
Lefeuvre, P., Lett, J.M., Reynaud, B., Martin, D.P., 2007. Avoidance of protein fold disruption in natural virus recombinants. PLoS Pathog. 3, e181.
McKenna, R., Bowman, B.R., Ilag, L.L., Rossmann, M.G., Fane, B.A., 1996. Atomic structure of the degraded procapsid particle of the bacteriophage G4: induced structural changes in the presence of calcium ions and functional implications. J. Mol. Biol. 256, 736–750.
McKenna, R., Ilag, L.L., Rossmann, M.G., 1994. Analysis of the single-stranded DNA bacteriophage phi X174, refined at a resolution of 3.0 A. J. Mol. Biol. 237, 517–543.

McKenna, R., Xia, D., Willingmann, P., Ilag, L.L., Krishnaswamy, S., Rossmann, M.G., Olson, N.H., Baker, T.S., Incardona, N.L., 1992. Atomic structure of single-stranded DNA bacteriophage phi X174 and its functional implications. Nature 355, 137–143.
Montville, R., Froissart, R., Remold, S.K., Tenaillon, O., Turner, P.E., 2005. Evolution of mutational robustness in an RNA virus. PLoS Biol. 3, e381.
Novak, C.R., Fane, B.A., 2004. The functions of the N terminus of the phiX174 internal scaffolding protein, a protein encoded in an overlapping reading frame in a two scaffolding protein system. J. Mol. Biol. 335, 383–390.
Pearson, V.M., Miller, C.R., Rokyta, D.R., 2012. The consistency of beneficial fitness effects of mutations across diverse genetic backgrounds. PLoS One 7, e43864.
Pepin, K.M., Domsic, J., McKenna, R., 2008. Genomic evolution in a virus under specific selection for host recognition. Infect. Genet Evol. 8, 825–834.
Rokyta, D.R., Joyce, P., Caudle, S.B., Miller, C., Beisel, C.J., Wichman, H.A., 2011. Epistasis between beneficial mutations and the phenotype-to-fitness Map for a ssDNA virus. PLoS Genet 7, e1002075.
Rokyta, D.R., Wichman, H.A., 2009. Genic incompatibilities in two hybrid bacteriophages. Mol. Biol. Evol. 26, 2831–2839..
Roux, S., Krupovic, M., Poulet, A., Debroas, D., Enault, F., 2012. Evolution and diversity of the Microviridae viral family through a collection of 81 new complete genomes assembled from virome reads. PLoS One 7, e40418.
Sackman, A.M., Reed, D., Rokyta, D.R., 2015. Intergenic incompatibilities reduce fitness in hybrids of extremely closely related bacteriophages. PeerJ 3, e1320.
Sackman, A.M., Rokyta, D.R., 2013. The adaptive potential of hybridization demonstrated with bacteriophages. J. Mol. Evol. 77, 221–230.
Sanger, F., Coulson, A.R., Friedmann, T., Air, G.M., Barrell, B.G., Brown, N.L., Fiddes, J.C., Hutchison, C.A., 3rd, Slocombe, P.M., Smith, M., 1978. The nucleotide sequence of bacteriophage phiX174. J. Mol. Biol. 125, 225–246.
Springman, R., Kapadia-Desai, D.S., Molineux, I.J., Bull, J.J., 2012. Evolutionary recovery of a recombinant viral genome. G3 (Bethesda) 2, 825–830.
Uchiyama, A., Chen, M., Fane, B.A., 2007. Characterization and function of putative substrate specificity domain in microvirus external scaffolding proteins. J. Virol. 81, 8587–8592.
Uchiyama, A., Fane, B.A., 2005. Identification of an interacting coat-external scaffolding protein domain required for both the initiation of phiX174 procapsid morphogenesis and the completion of DNA packaging. J. Virol. 79, 6751–6756.
Wichman, H.A., Badgett, M.R., Scott, L.A., Boulianne, C.M., Bull, J.J., 1999. Different trajectories of parallel evolution during viral adaptation. Science 285, 422–424.
Wichman, H.A., Brown, C.J., 2010. Experimental evolution of viruses: microviridae as a model system. Philos Trans. R. Soc. Lond. B Biol. Sci. 365, 2495–2501.
Wichman, H.A., Millstein, J., Bull, J.J., 2005. Adaptive molecular evolution for 13,000 phage generations: a possible arms race. Genetics 170, 19–31.
Wichman, H.A., Scott, L.A., Yarber, C.D., Bull, J.J., 2000. Experimental evolution recapitulates natural evolution. Philos Trans. R. Soc. Lond. B Biol. Sci. 355, 1677–1684.